DENSIFICATION AND ELECTROPHORETIC DEPOSITION (EPD) ON TI6AL4V SUBSTRATE USING BIOGLASS®

SUMMARY

The goal of this article is to show the possibility to coat Ti6Al4V substrates with bioglass powder by means of electrophoretic deposition (EPD), subsequently followed by a suitable heat treatment to densify the coating.
Smooth defect free thick (> 1 mm) coatings were obtained on anodised Ti6Al4V cylindrical substrates by means of EPD. The voltage, powder concentration and time during EPD are important to produce coatings with the wanted thickness.
EPMA and XRD analysis were performed on the densified coating and revealed that the bioglass phase was transformed to a crystalline phase.

KEYWORDS: Titanio, vidrio Bioactivo, Deposición Electroforetica, Recubrimiento Sinterizado, Microondas.

JORGE LUIS ENCISO MANRIQUE
Ingeniero Metalúrgico, M.Sc ingeniería de Materiales.
Director Grupo de investigación GIMAP.
Profesor Universidad de Ibagué
jlenciso@nevado.cui.edu.co

ABSTRACT

El objetivo de este articulo es mostrar la posibilidad de recubrir titanio Ti6Al4V con polvos de vidrio bioactivo (45S5) por medio de deposición electroforetica (EPD) seguido de un tratamiento de densificación del recubrimiento.
Superficies suaves y libres de defectos fueron obtenidas (> 1mm) sobre un cilindro anodinado de Ti6Al4V por medio de EPD. El voltaje, la concentración de polvos y el tiempo durante el EPD son importantes para producir recubrimientos con espesores deseados. Análisis de EPMA y XRD fueron realizados sobre el recubrimiento densificado y revelo la transformación de fase del vidrio bioactivo en una fase cristalina.

KEYWORDS: Titanium, Bioglass, Electrophorectic Deposition, Sintering, Coating, Microwave.

1. INTRODUCTION

One of the limiting factors, affecting widespread application of bioglass is the difficulty on producing well-adhering coating by and industrial feasible process. Different processes are possible for the deposition of a bioactive glass layer on titanium substrates like plasma spraying, chemical vapour deposition, dip coating, electrophoretic deposition (EPD) and electrochemical deposition. The coating process not only influences the cost of the processing, but will also the coating structure, the adhesion with the substrate, the porosity (shape, size morphology), and in this way the bioactivity.

The method, which will be investigated here to coat Ti6Al4V substrates with bioglass, is electrophoretic deposition. This is a process in which suspended charged powder particles are deposited on an electrode under influence of an electric field. Some advantages of this technique are high reproductivity, low cost, and the high speed. EPD can produce coatings with a broad thickness from less than 1µm to more than 500µm [1], while deposition rates vary from seconds to minutes offering an easy control over the thickness and morphology of the coating.

After electrophoretic deposition the obtained coating, which is in fact still a powder compact, has to be densified by a heat treatment. In this work microwave sintering will be investigated. In microwave sintering, electromagnetic waves interact with ceramic materials, leading to volumetric heating by dielectric loss. Such a volumetric heating can help to improve the problems given with conventional heat transfer and to generate a more uniform microstructure [2].

2. TITANIUM ALLOYS

Ti already exists as a biomaterial for more than 60 years. Due to strength properties, titanium was replaced by one of its alloys: Ti6Al4V, which is today's most used implant material [3]. Due to the formation of a stable oxide surface, Ti is one of the most biocompatible metals. It is mainly used for orthopaedic and oral implants thanks to the high corrosion and fatigue resistance, a relative low E-modulus compared to bone, a high strength/weight-relationship and a relatively high hardness [4].
Titanium exists in two crystallographic phases: a low temperature alpha (α) phase, which has a close-packed hexagonal (c.p.h.) crystal structure, and a high temperature beta (β) phase that has a b.c.c. structure. To provide a wide range of useful mechanical property

Fecha de Recepción: 31 Agosto de 2006
Fecha de Aceptación: 24 Noviembre de 2006

combinations, the morphology of these two allotropic phases has to be manipulated through alloy elements and thermo-mechanical processing [5]. Different microstructures are possible: α-, α/β-, β-alloys, and the intermetallics (TixAl, where x = 1 or 3). Alloying elements can be divided into substitutional (molybdenum, vanadium, manganese, etc) and interstitial (oxygen, nitrogen and hydrogen) solutes [6]. The ranges and effects of different alloying element used in titanium are shown in table 1. A number of authors [7] agree about two mayor divisions of stabilised systems: α and β, Molchona [ASM handbook, 2000] has developed a convenient categorisation of titanium phase diagram. Titanium alloys like Ti6Al4V present a α/β structure, retaining more β-phase, which affects the properties (i.e. when Ti6Al4V is cooled from high temperatures it can transform the β-phase in a coarse acicular structure or a fine acicular α structure through a diffusion-controlled nucleation and growth mechanism depending on the cooling rate).
Generally, acicular α improves creep resistance, fracture toughness and crack growth resistance, but loosing ductility and fatigue. When the transformed β structure is coarse, toughness and crack-growth resistance are improved and ductility and fatigue strength are reduced [5].

Alloying element	Range Wt%	Effet on structure
Aluminium	3-8	α stabiliser
Tin	2-4	α stabiliser
Vanadium	2-15	β stabiliser
Molybdenum	2-15	β stabiliser
Chromium	2-12	β stabiliser
Copper	± 2	β stabiliser
Zirconium	2-5	α and βstabiliser
Silicon	0.05-0.5	Improves creep resistance

Table 1. Ranges and effects of some alloying elements used in titanium.

3. BIOGLASS (45S5)

Bioglass is characterised by its behaviour and special composition that increases the bonding. The surface forms a biologically active hydroxyapatite layer, which gives a bonding interface, forming a phase that is chemically and structurally equivalent to the bone phase.

Bioglass (45S5) has a general composition of 45% wt SiO_2, 6% wt P_2O_5, 24.5% wt CaO, and 24.5% wt Na_2O. Compositions with 45-55% of SiO_2 will join to the collagen of smooth tissues with the bone, and bioglass containing about 55-60% of SiO_2 will only join to the bone. The compositional dependence (in wt %) of bone-bonding and soft-tissue bonding for Na_2O-CaO-P_2O_5-SiO_2 glasses. All glasses contain a constant 6wt% of P_2O_5 [9].

4. ELECTROPHORETIC DEPOSITION (EPD)

Electrophoretic deposition (EPD) is very promising because it is a fairly rapid, low cost process for the fabrication of ceramic coatings, monoliths, composites, laminates and functionally graded materials varying in thickness from a few nanometers up to centimetres [10]. Nowadays, coatings are world-wide processed by electrophoretic deposition for phosphor screens, oxygen sensors, fuel cells, photo-chemical cells, solar cell applications, etc. Most papers report on the possibility to deposit coatings between nm scale and 200 μm on porous or dense substrates [11]. However, the main problem associated with this process is often the difficulty to densify the coatings without cracking.

Electrophoretic deposition consists of two processes, i.e. the movement of charged particles in suspension in an electric field between two electrodes (electrophoresis) and particle deposition on one of the electrodes (see figure 1) or onto a membrane (electro-coagulation).

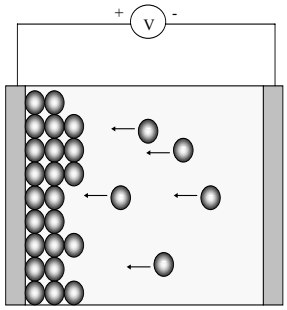

Figure 1. Schematic view of the EPD process

After EPD, a powder compact with a green density between 40 and 60 % of the theoretical density is obtained, which needs to be fully densified by sintering or curing. EPD requires a stable suspension in which the powder particles must carry a sufficient charge. A suspension is termed stable if the particles experience a repulsive force when they approach each other, so that agglomeration is avoided. Hence, more defect-free deposits can be formed from such suspensions as the incorporation of aggregates is avoided. Four mechanisms have been identified by which the charge on the particles can develop [10].

(i) Selective adsorption of ions from the liquid phase onto the solid particle,
(ii) Dissociation of ions from the solid particle into the liquid,
(iii) Adsorption of dipolar molecules on the particle surface,
(iv) Electron transfer between the liquid phase and the solid particle.

The exact mechanism of deposition at the electrode is still not entirely clear. Up to now, different possible mechanisms have been proposed in literature.

In general, the EPD process can be applied to materials that have an adequate shape for the deposition using fine powders (< 30 μm) that present good adhesion once they are sintered [ASM, 2002].

Controlling the kinetics is of primary importance during electrophoretic deposition. Hamaker experimentally derived an equation, which states that the amount of powder brought to the electrode during a time follows [12]:

$$\frac{dY}{dt} = f\,\mu\,E\,c\,A \qquad (1)$$

With Y: yield of deposition (g),
t : deposition time (s),
E: electric field strength (V/m),
A: surface area of the electrode (m²),
c : solids loading in suspension (g/m³),
μ : electrophoretic mobility (m²/V.s).
f :a factor taking into account that not all powder that moves to the electrode is necessarily incorporated in the deposit.
After deposition with bioglaas power the samples shows a good homogeneity without cracks Figure 2

Figure 2. Sample coated with bioglass (45S5) by EPD

.

5. CHARACTERISATION METHODS

5.1 Characterisation of suspensions

Zeta potential measurements

Electrophoretic mobility and zeta potential measurement in concentrated suspensions were performed with the electro-acoustic measuring technique (ESA 8000, MATEC). The mobility was measured via Electroacoustic Sonic Amplitude (ESA) directly in the suspension to which n-butylamine or nitrocellulose was added stepwise with a titration.

The dynamic mobility, μ_d, is preferred over the ESA-signal, as it represents a value, which is independent from the solids loading of the suspension. It is possible to convert μ_d, to the ξ-potential with

$$\mu_d = \frac{2\varepsilon\xi}{3\eta}\cdot(1+f)\cdot G(\alpha) \qquad (2)$$

With

$$G(\alpha) = \left(\left[1-\frac{1}{9}\left(\frac{\omega r^2\rho}{\eta}\right)\left(3+2\frac{\Delta\rho}{\rho}\right)\right]\Big/\left[1+(1+i)\left(\frac{1}{2}\frac{\omega r^2\rho}{\eta}\right)^{1/2}\right]\right)^{-1} \qquad (3)$$

With

ε : the dielectric number of the dispersing medium [-]

ξ : The ξ-potential [V]

η : the viscosity of the dispersing medium [Pãs]

f: f = 0 for apolar and f = 0.5 for polar media [-]

ω : the frequency during measurement [s^{-1}]

r: the particle radius [m]

$\Delta\rho$: the difference of the densities between particles and liquid [kg/m^3]

ρ : the particle density [kg/m^3]

For particles smaller than 1μm, the dynamic mobility and the electrophoretic mobility are the same.

5.2 EPD - kinetics

Theory

To predict the coating thickness in function of the time, Hamaker's equation [12] is used to describe the kinetics of the EPD process:

$$\frac{dY}{dt} = f\cdot\mu\cdot c\cdot E\cdot S \qquad (4)$$

with the yield Y (kg), time t (s), the electrophoretic mobility μ (cm²/V.s), the electrical field strength E (V/m) between the electrodes, the solids loading C (kg/m³) of the powder in suspension and the surface area A (m²) of the electrode, f is a factor which takes in account that not all powder brought to the electrode is incorporated in the deposit. In this work, f is assumed to be 1. In this equation the electric field strength has to be known. [13] found that a potential drop can be created at the depositing electrode or over the deposit, but the extend of this potential drop is determined by the solvent and charging agents. It was found that for suspensions based on methyl ethyl keton and n-butylamine the electric field strength during EPD is constant and no potential drop at the electrodes happened.

For an electrode set-up with flat shaped electrodes, the electric field strength is equal to:

$$E = \frac{V_{applied}}{d} \qquad (5)$$

With d the distance between the electrodes and $V_{applied}$ the applied voltage.

The powder concentration c (kg/m^3) can also be written in function of the thickness d_1 of the powder compact at the electrode:

$$c = \frac{M - Y}{H - d_1 S} \tag{6}$$

With M the amount starting powder (kg), H suspension volume (m^3).
If d_1 is very small compared with d, equation (2) can also be written as:

$$\frac{dY}{dt} = k\left(\frac{M - Y}{H}\right) \tag{7}$$

With $k = f\ \mu\ E\ S$ (8)

The solution of this differential equation is

$$Y = M(1 - e^{-kt/H}) \tag{9}$$

From this equation, the factor k can be calculated and in this way the electrophoretic mobility.

For a cylindrical electrode set-up, the electric field strength has to be changed by:

$$E = \frac{V_{applied}}{a\left(\ln(\frac{b}{a})\right)} \tag{10}$$

With $V_{applied}$ the applied voltage, b the radius of the counter-electrode, the radius of the deposition electrode.

In order to investigate the amorphous character of the bioglass powder, XRD analyses were carried out on powder compacts. 2θ was varied between 20 and 90° (figure 3). Only one broad peak was detected around 30°. This peak is the amorphous silica peak [14]. It is clear that the powder is amorphous because no other peaks were obtained.

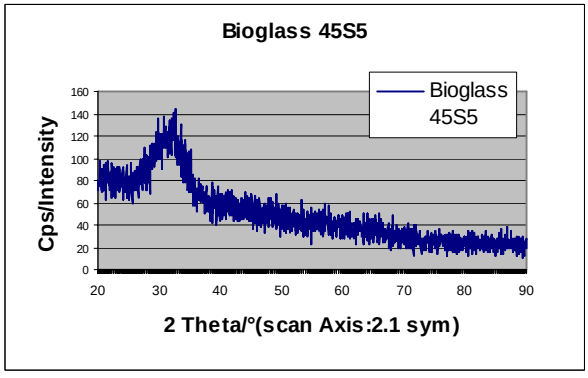

Figure 3. XDR spectrum of the bioglass powder.

The morphology and shape of the powder was analysed by means of SEM, as illustrated in Figure 4. From the SEM pictures, it is observed that the bioglass particles are very angular and have a platelet shape.

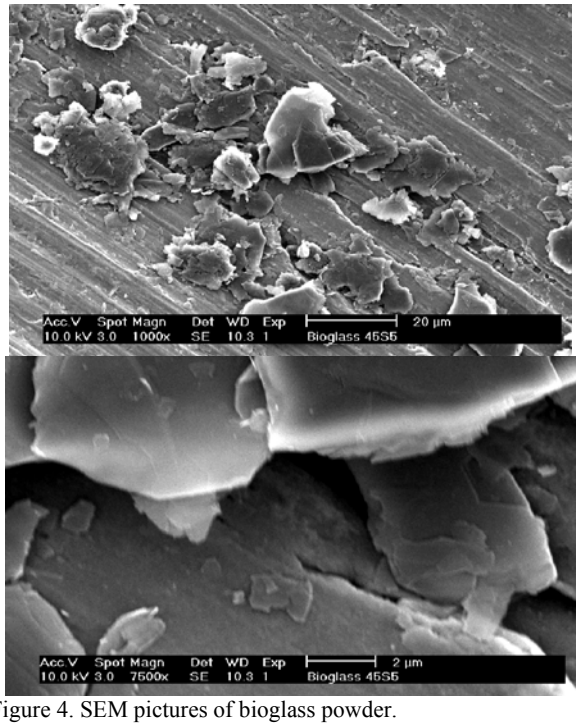

Figure 4. SEM pictures of bioglass powder.

6. MICROWAVE SINTERING

Ceramic sintering is an attractive area of microwave processing; the advantages of this process include rapid heating rates, short processing times, low power requirements and reduced reaction with the atmosphere [2]. Microwave heating is fundamentally different from conventional heating. The heat is in fact generated within the sample and transported from the sample to the environment (figure 5).

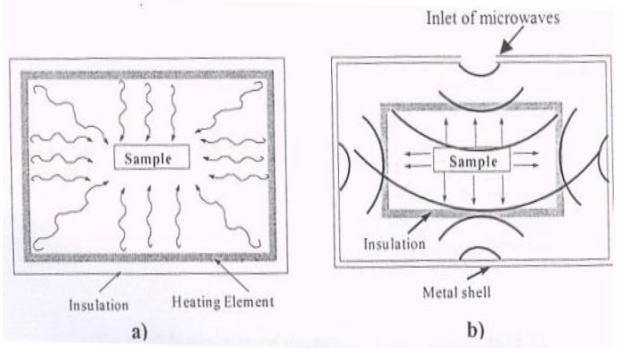

Figure 5. Heating samples in a conventional (a), and microwave furnace (b).

Microwaves are electromagnetic radiation with wavelengths ranging from 1 mm to 1 m in free space with a frequency between 300 GHz to 300 MHz. Today, microwaves at the 2.45 GHz frequency are used almost universally for industrial and scientific applications.
The microwave mechanism is based on the interaction between microwave and materials. The power absorbed by a material exposed to microwaves is proportional to its dielectric loss factor [2].

$$P = 2\pi f \varepsilon_0 \varepsilon'' E^2 \qquad (11)$$

Where P is the power absorbed per unit volume, f, the frequency of microwaves, ε_0 the

Dielectric constant in free space, ε'', the dielectric loss factor, and E, the internal electric field.

The loss factor normally increases exponentially with temperature and determines the classification of materials. These materials are classified in four groups: transparent (low loss insulator), opaque (conductor), absorber (lossy insulator) and mixed. When a MW transparent material is subject to MW radiation for long time it should be heated up slowly. This factor is undesirable not only because of the time consumption, but also because of the risk of plasma formation.
Materials with a high loss tangent can couple with microwave at room temperature (carbon, silicon, carbide and vanadium oxide), while the lower dielectric loss material, such as zirconia and alumina need a higher initial temperature in order to couple.
To ensure the coupling at low temperature, *Hybrid Microwave Sintering* can be used. In this set-up, a susceptor is placed around the sample. This susceptor couples at low temperature with the microwaves, generates heat, which warms up the sample to the temperature at which it also couples with microwaves.

6.1 Homogeneity of the coating

The homogeneity parallel and perpendicular with the substrate material was investigated.
Figures 6 show a detailed SEM picture of the coating surface. A rough surface is observed in which the initial powder particles are still visible.

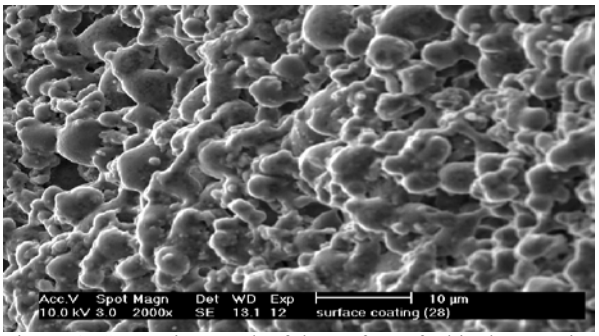

Figure 6. SEM micrograph of the surface of a bioglass coating, densified by microwave sintering

During sintering a graded interaction zone can be created between the coating and the substrate material. This composition of the interaction zone influences the local thermal expansion coefficient and in this way the final residual stress state. Therefore composition profiles were measured by means of EPMA along a cross-sectioned coated substrate after respectively a first and second sintering step (see figures 7). The second sintering was performed to increase the thickness, improving the adhesion and porosity of the coating. Analysis was performed, based on the following oxides: TiO_2, SiO_2, CaO, P_2O_5.

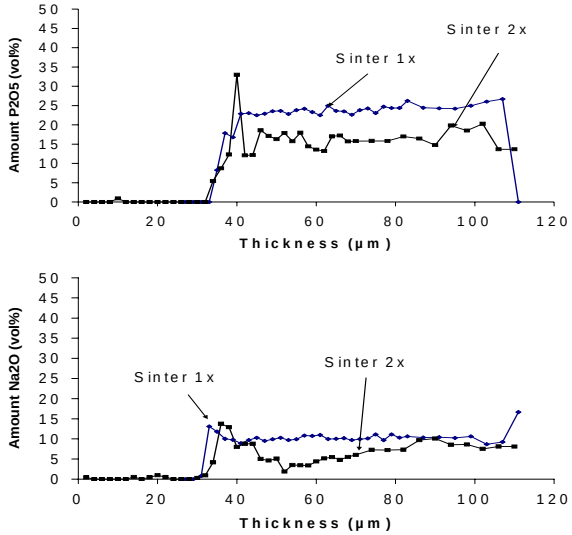

Figure 7. Composition profile over the coating at respectively 1x and 2x microwave sintering cycles.

From the composition profiles, it was found that an interaction zone exists between the substrate and bioglass. The width of the interaction zone is the same for a first and second sinter cycle, but the width of the diffusion layer is dependent for the analysed elements.

6.3 Cristallinity of the bioglass coating

By means of XRD the crystalline character of the coating was investigated. As already was discussed in paragraph x, the as deposited powder showed an amorphous character.
After sintering in the microwave with the optimal inters parameters, the amorphous character of the coating disappeared. There are clearly peaks presents in the spectrum $2\theta = 20°\text{-}90°$ of some crystalline phase. One of the requests of a bioactive glass layer is the amorphous character [15] of the glass phase. This is not the case and in the future experiments care has to be taken to maintain the amorphous character. Increasing the cooling speed after sintering can perform this below the glass transition temperature. Above this temperature a slow cooling speed is necessary to maintain the equiaxial structure of the substrate material (figure 8).

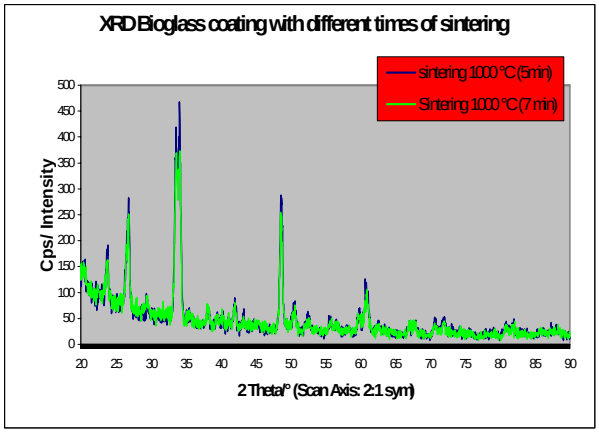

Figure 8. XRD of bioglass (45S5) coating with sintering times of 5 and 7 min; c) second sintering.

7. CONCLUSIONS

A suspension based on methyl ethyl keton, n-butylamine and nitrocellulose was a suitable suspension to obtain very smooth bioglass coatings. After drying crack free deposition of more than 1 mm were obtained, but these thick coatings couldn't be successfully sintered. The absence of cracks was attributed to the shape of the particles.

The heat treatment also affected the microstructure of the substrate material. An equiaxial α/β was present after a sinter treatment in the microwave furnace, but a wildmanstätten structure was present after a second heat treatment in the microwave furnace. Also the hardness was slightly higher after a heat treatment.

Characterisation of the coatings made by microwave sintering showed that an interaction zone was present between substrate and coating, but the thickness was not influenced by the amount of heat treatments. This was also translated in a rather good adhesion between substrate and coating.

XRD analysis were performed on the densified coating and revealed that the bioglass phase was transformed to a crystalline phase.

Because EPD of bioglass gave no real problem, the suggestions for future work are more concentrated on the heat treatment. So is it necessary to optimise the heat treatment:

- to obtain more amorphous bioglass
- to control crack formation
- to control the microstructure of the substrate

Las conclusiones son obligatorias y deben ser claras. Deben expresar el balance final de la investigación o la aplicación del conocimiento.

8. BIBLIOGRAPHY

[1] Put S., "Functionele gradient materialen aangemaakt met behulp van elektroforetische depositie", Proefschrift ter behaling van pH. Degree at MTM. 2003.

[2] Chao Z., "Functionally graded Ce-ZrO2-based composites", Katholieke Universiteit Leuven, 1999.

[3] Kokubo T., Kim H. M., Kawashita M., Nakamura T., "Bioactive metals: preparation and properties"., Journal of Materials Science: materials in medicine 15, 99-107, 2004.

[4] Cooper L. F."A role for surface topography in creating and maintaining bone at titanium endosseous implants", the journal of prosthesis dentistry, vol. 84, number 5, November 2000.

[5] Caron R. N. Olin Corporations; Staley J. T. Alcoa Technical Center, "Effect of composition, processing, and structure on properties of non-ferrous alloys", ASM, 2002.

[6] Froes. F.H, "Titanium alloys properties and applications", science and Technology, ISBN: 0-08-0431526, 9367 – 9369, Elsevier Science, 2001.

[7] Boyer R, Welsh G, and Collin EW, Materials properties Hand Book, Titanium Alloys, ASM international, 1994.

[9] Hench L., "Biomaterials: a forecast for the future", Biomaterials 19, 1419- 1423, Elsevier, 1998.

[10] Van der Biest O., Vandeperre L.,"Electrophoretic deposition of materials" Annu. Rev. Mater. Sc. 199. 29-327-52, 2002.

[11] Put S., "Literature review on electrophoretic deposition of hydroxyapatite coating on titanium-bases substrates". Katholieke Universiteit Leuven, 2003.

[12] Hamaker H, "Trans Faraday" Soc 36, 279, 1940

[13] Van der biest O., Put S., Anne G., Vleugels J., " Electrophoretic deposition for coating and free standing objects", Journal of Materials Science 39, 779-785, 2004.

[14] Leonelli C., Lusvardi G., Malavasi G., Menabue L., Tonelli M., "Synthesis and characterisation of cerium-doped glasses and in vitro evaluation of bioactivity", Journal of Non- Crystalline Solids 316, 198-216, 2003.

[15] Schrooten J., Roebben G. and Helsen J. A., "Yougn's modulus of bioactive glass coated oral implants: Porosity corrected bulk modulus versus resonance frequency analysis", Scripta Materialia, Volume 41, No. 10, pp 1047-1053, 1999.

[16] Hench L., " Bioceramics" J.Am, Ceramic Soc., 81 (7), 1705-28, 1998.

[17] Mochona, ASM Handbook, 2000

[18] Prado da Silva M. H., Soares G. A., Elias C. N., Lima J.H.C., Shechtman H., Gibson I. R., Best S. M., "Surface analysis of titanium dental implants with different topographies", Materials research, vol. 3, No 3, 61-67, 2000.